

COMPARISON OF DIFFERENT RELATIVE MOVEMENT DIRECTIONS OF MAGNET AND COIL IN AN ELECTROMAGNETIC ENERGY HARVESTER

B. Mack, M. Stürmer, U. Wallrabe

Laboratory for Microactuators, Department of Microsystems Engineering (IMTEK),
University of Freiburg, Germany

Abstract: This paper investigates the effect of the relative position of magnet and coil in an electromagnetic energy harvester on the converter's output. Both the moving direction and the north-south orientation (NS-orientation) of the magnet are varied. The open-circuit voltage delivered by the converter when it is excited sinusoidally by a shaker table is used to compare the different situations. Referring to the direction of the normal vector of the cylindrical coil it could be shown for our geometrical setup that the parallel NS-direction combined with the parallel movement of the magnet yields the maximum output voltage for the investigated frequencies.

Key words: vibration energy harvesting, electromagnetic, moving direction, north-south-direction

1. INTRODUCTION

Environmental vibrations are a possible energy source for Energy Harvesting (EH). For the scavenging of vibrations which has been previously reported in e.g. [1][2][3] three mechanisms are possible: electrostatic, piezoelectric and electromagnetic. This work is dealing with the electromagnetic approach.

In an electromagnetic generator a permanent magnet and a coil vibrate with respect to each other inducing a voltage according to Faraday's law of induction. This relative movement arises only from inertia. Therefore a bigger inertial mass will result in a greater voltage or power output of the device. If the permanent magnet has a bigger mass than the coil it is favourable to use the magnet as inertial mass rather than the coil. Given coil and magnet, for maximization of the voltage the change of the magnetic flux through the coil in time has to be chosen as large as possible. With view to a miniaturization and parallelization it is the scope of this paper to investigate diverse coil-magnet assemblies which may appear unconventional from a classical macroscopic view point but meaningful in terms of micro manufacturing, such as in plane movement, e.g..

Because of its high remanent flux density NdFeB is a suitable permanent magnetic material.

2. DESCRIPTION OF INVESTIGATIONS

In order to investigate the influence of the movement direction and the orientation of the magnet we have assembled a laboratory set-up of an energy harvester. A simple arrangement is chosen which allows for subsequent miniaturization with MST technologies.

Four movement situations of the magnet are shown in figure 1a to d. The normal vector of the cylindrical coil denotes the z -direction. Changing the orientation of the magnet before fixing it to the cantilever results in diverse movement directions as shown in figure 2.

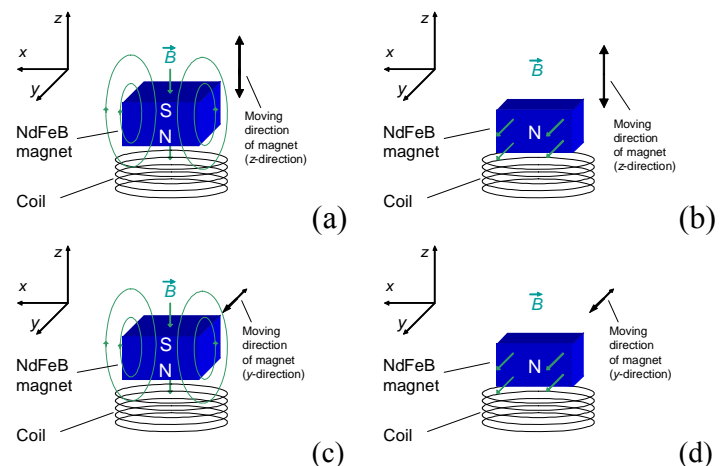


Figure 1. Investigated movement directions of the magnet referring to the normal vector of the coil. (a): movement and NS-direction parallel, (b): movement parallel and NS-direction perpendicular, (c): movement perpendicular and NS-direction parallel, (d): movement and NS-direction perpendicular.

The movement of the magnet in z -direction (figure 2a and b) will be referred to as parallel movement because it is parallel to the orientation of the coil. The movement of the magnet shown in figure 2c and d will be referred to as perpendicular movement, vice versa. For the perpendicular movement both magnet and coil have to be rotated by 90° compared to the parallel movement (compare figure 2c and d with 2a and b).

In addition to the movement direction different rest positions of the magnet are investigated. For the case of parallel movement the rest position of the magnet will be varied in z -direction. For the case of perpendicular movement the rest position of the magnet will be varied in y -direction. In any case the specification of the rest position requires 3 Cartesian coordinates.

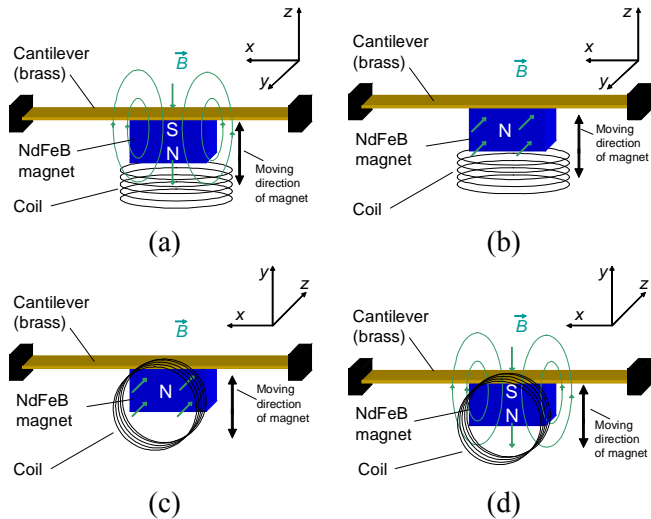


Figure 2. Experimental realizations of the movement directions shown in figure 1a, b, c and d, respectively.

3. DEVICE AND EXPERIMENTAL SETUP

A photo of the laboratory set-up is depicted in figure 3. The magnet is attached to a brass cantilever of size $0,3 \times 10,0 \times 134,7 \text{ mm}^3$. The coil is wrapped in sticky tape for fixation, hence it can not be seen directly. Apart from the magnet itself all parts are made of non-ferromagnetic material. The whole device is placed on a shaker table where it is excited sinusoidally with a defined amplitude and frequency.

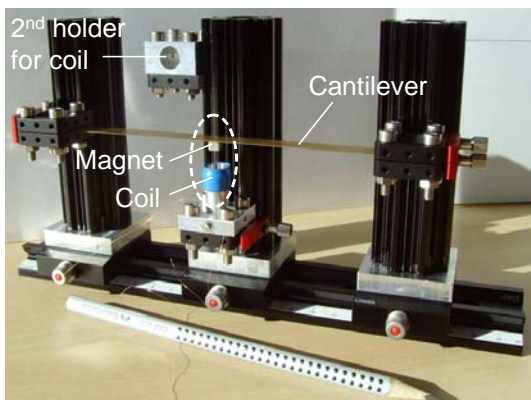


Figure 3. Laboratory set-up for the case of parallel movement.

For parallel movement the relative position of the magnet and the coil can be varied with a precision of 0,5 mm in x - and z -direction whereas it is fixed in y -

direction. For perpendicular movement the relative position can be adjusted with a precision of 0,5 mm in each direction using a scale on the guide rails or a spacer with defined thickness.

In the experiment a 50 μm thick insulated copper wire is wound around a hollow aluminium cylinder with an outer diameter of 10 mm. The resulting coil with a diameter of 10 mm has 50 windings distributed over a length of $l_{\text{coil}} = 4 \text{ mm}$. In the direction of the magnet the cylinder extends $d_1 = 1 \text{ mm}$ in front of the coil (see figure 4). The measured resistance of the coil is $R_c = 7 \Omega$ and its calculated inductance is approximately $L = 62 \mu\text{H}$ large.

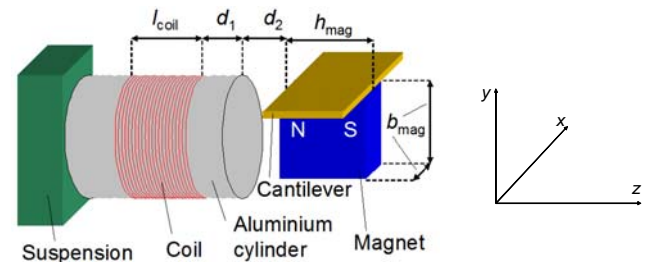


Figure 4. Schematic description of the relative distances of coil and magnet for the situation of figure 2c. The other three situations look analogue, h_{mag} is always the extension of the magnet in NS-direction.

The total expansion of the NdFeB magnet with a 15 μm thick Zn-Ni-coating is 4,5 mm in NS-direction and 4,8 mm in both other dimensions. The magnetic flux density B_w was simulated with COMSOL along straight lines parallel to the NS-direction which are numbered 1 to 5 in figure 5. To verify the simulation B_w was also measured on the symmetry axis of the magnet in NS-direction using a fluxmeter. The results are also plotted in figure 5. Simulation and measurement are in good agreement.

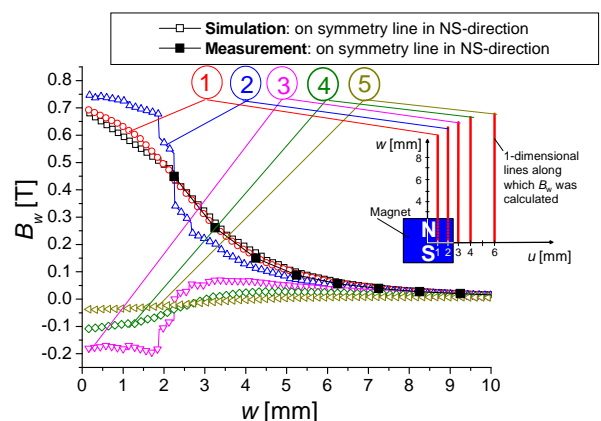


Figure 5. Simulation and measurement of the flux density B_w along straight lines parallel to the NS-direction. The magnet's centre is in the u - w -plane.

From figure 5 we observe the largest gradients of B_w in the region $1.5 \text{ mm} < w < 3.5 \text{ mm}$, independently of the distance of the line to the magnet. The sign of the gradients in this region, however, depends on the distance to the magnet (see figure 5). So if the magnet is moving in a coil and we assume the w -axis to be parallel to the normal vector of the coil then at certain positions the opposite signs of the gradients will lead to a reduced flux change through the coil windings and thus to a smaller induced voltage. Consequently, for a reasonable evaluation it is necessary to calculate the total flux through the coil for different positions of the magnet. Then we are able to estimate the optimum rest position of the magnet which yields the maximum output voltage when the magnet is vibrating.

4. SIMULATIONS

For the two situations shown in figure 1a and c the magnetic flux through the coil was calculated for different rest positions of the magnet using the software COMSOL. It is assumed that the density of the coil's windings is homogeneous, the diameter of all windings is 10 mm. Furthermore we use $l_{\text{coil}} = 4 \text{ mm}$ for the calculation. In the following z is the distance of the coil's and the magnet's centre.

Let us first take the moving situation of figure 1a. Starting at $z = 0$, with increasing z the magnetic flux through the coil will decrease. This behaviour can be seen in figure 6. At approximately $z = 3 \text{ mm}$ the slope becomes maximum. This means that the induced voltage is maximum when the magnet is vibrating while its rest position is chosen to be at $z = 3 \text{ mm}$.

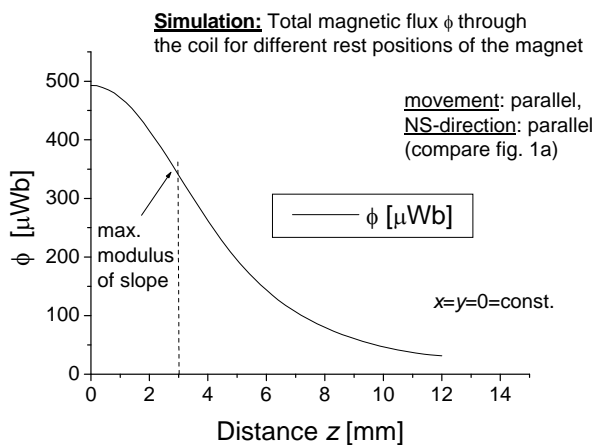


Figure 6. Total magnetic flux through the coil at different rest positions of the magnet for the situation in figure 1a.

A similar calculation may be done for the situation in figure 1c. Here y is the distance between the perpendicular bisecting line of the coil and the magnet's centre. Figure 7 shows the simulation result for

$x = 0 = \text{const.}$ and $z = 6 \text{ mm} = \text{const.}$ Clearly, for $y = 0$ the flux through the coil has to be maximum and it is symmetric for negative and positive y values. The slope is maximum at $y = \pm 4,2 \text{ mm}$ which logically are the rest positions at which the maximum voltage can be expected when the magnet is vibrating.

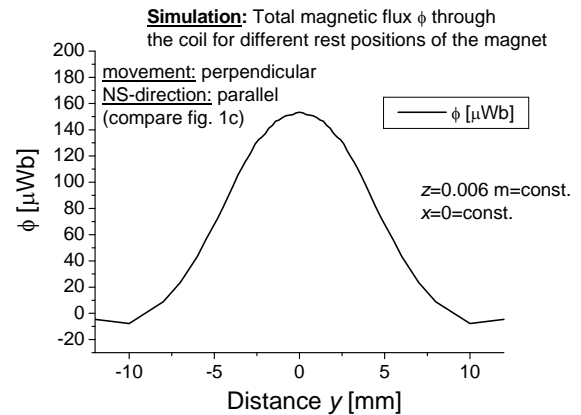


Figure 7. Total magnetic flux through coil at different rest positions of the magnet for the situation in figure 1c.

5. MEASUREMENT RESULTS

First, the situations in figure 1a and b are compared. The rest position of the magnet is varied along the coil's symmetry axis in z -direction and the open-circuit voltage is measured. figure 8 and 9 show the measured open-circuit voltage as a function of z at diverse frequencies for the situations of figure 1a and b, respectively. Each measurement has been repeated six times using different beams and different restraints in order to account for the corresponding uncertainties. The measured voltage in figure 8 is maximum at $z = 3 \text{ mm}$ as was predicted from the maximum of the flux gradient in the simulation of figure 6.

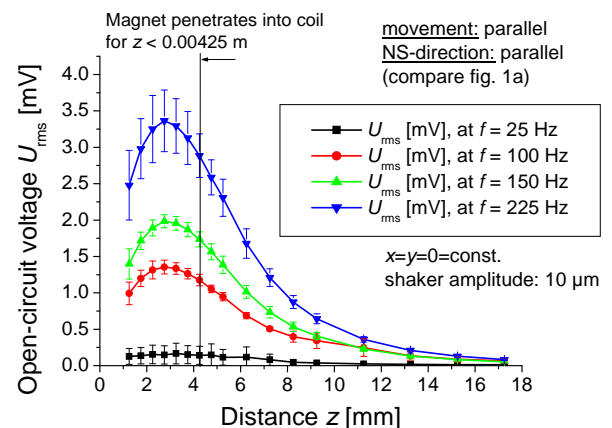


Figure 8. Measured open-circuit voltage U_{rms} over rest position z between the centre of the magnet and the centre of the coil (moving situation: figure 1a).

Within the observed errors the moving magnet from figure 1a yields a higher voltage compared to the case from figure 1b for the investigated frequencies. Similar measurements were performed for perpendicular magnet movement. Here, we do not observe mentionable differences in the achievable voltages between the parallel and perpendicular NS-direction.

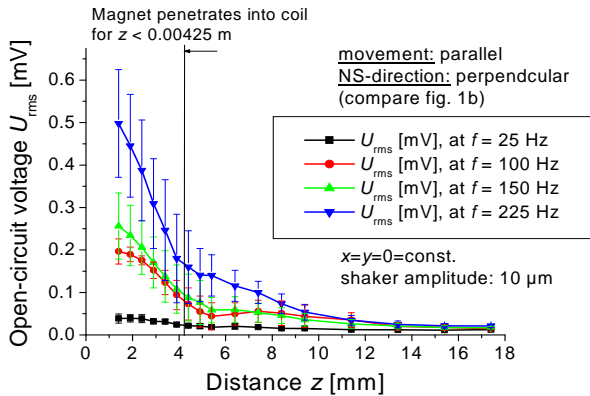


Figure 9. Measured open-circuit voltage U_{rms} over rest position z between the centre of the magnet and the centre of the coil (moving situation: figure 1b).

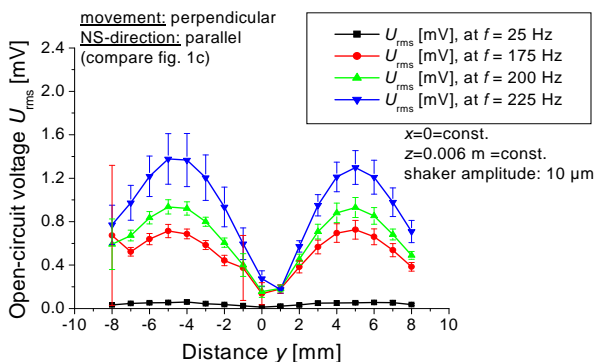


Figure 10. Measured open-circuit voltage U_{rms} over rest position y between the centre of the magnet and the perpendicular bisecting line of the coil (moving situation: figure 1c).

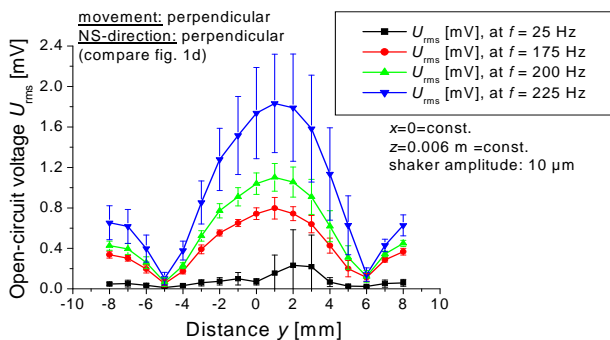


Figure 11. Measured open-circuit voltage U_{rms} over rest position y between the centre of the magnet and the perpendicular bisecting line of the coil (moving situation: figure 1d).

For symmetry reasons we would expect all curves in figure 10 and 11 to be symmetric to $y=0$. In the measurements the vertical symmetry line of some curves is shifted towards $y = 1$ mm. This is related to an adjustment accuracy of coil and magnet of 0,5 mm to 1 mm. Considering this shift the measurement is consistent with the simulation (compare figure 10 and figure 7).

6. CONCLUSION AND OUTLOOK

In this work we investigated the output voltage of an electromagnetic energy converter in dependence on the relative movement direction and the NS-orientation of a magnet with respect to the normal vector of the coil. For the NS-orientation and the magnet movement being parallel the maximum output voltage was reached. Furthermore the magnet has to immerse into the coil for an optimum output. For a prospective miniaturization several consequences follow for the construction of a micro device: The spring has to be designed in a way allowing the magnet to immerse into the coil without limiting the penetration because of the magnet's movement. For the same reason, the coil diameter needs to be greater than the magnet's extension. Third, many windings have to be close to the magnet. Thus the coil length must not exceed the magnet size or the vibration amplitude, depending on whether the magnet or its vibration amplitude is the greater. To still have many windings, coils with more than one layer of windings need to be fabricated. All these requirements can be fulfilled by a 3D cylindrical coil or, if the coil length is very small, by a quasi 2D coil with as many windings. To summarize the results, a high design and 3D fabrication effort is advantageous. This only makes sense when low cost processes, such as replication techniques, are used.

7. REFERENCES

- [1] Roundy S, Wright P K, Pister K S J, Micro-electrostatic vibration-to-electricity converters, *Proc. IMECE2002 (New Orleans, Louisiana, 2002)*
- [2] Stark B H, Mitcheson P D, Miao P, Green T C, Yeatman E M and Holmes A S, Power Processing Issues for Micro-Power Electrostatic Generators, *35th Annual IEEE Power Electronics Specialists Conference (Aachen, Germany, 2004)*
- [3] Pan C T, Wu T T, Development of a rotary electromagnetic microgenerator, *Jour. Micromechanics and Microengineering*, **17** 120-128, 2007